

Detection of Cavitation in Centrifugal Pumps

¹A.A.B. Al-Arabi, ²S.M.A. Selim, ³R. Saidur, ⁴S.N. Kazi, ⁵G.G. Duffy

¹Mechanical Engineering Department, Higher Institute of Engineering, Hoon, Libya.

²Faculty of Engineering, Minoufiya University, Shibin, El-Kom, Egypt.

^{3,4}Department of Mechanical Engineering, Faculty of Engineering, University of Malaya, 50603 Kuala Lumpur, Malaysia.

⁵Department of Chemical and Materials Engineering, School of Engineering, University of Auckland, Private Bag 92019, Auckland, New Zealand.

Abstract: Pumps are designed and manufactured to operate well away from the cavitation condition and thus the factors affecting the onset of cavitation are important. A specially designed test rig was constructed so that the onset of cavitation could be studied visually while obtaining actual NPSH data. The magnitude of the NPSH level at 3% drop in total discharge head of a pump was determined at different operating conditions. Photographs were obtained with a high speed camera indicated that the state of cavitation existed long before the pump performance was affected, and well before the 3% drop in total discharge head criterion was applied. Correlations between the calculated NPSH at the visual sighting of the onset of cavitation and NPSH values corresponding to a 3% drop in total discharge head were predicted at various operating conditions. Flow visualization as expected revealed that the intensity of cavitation varied according to the operating conditions (flow rate ratio, pump rotational speed, and water temperature).

Key words: Cavitation inception, NPSH, flow rate, visualization.

INTRODUCTION

Pump cavitation is caused by the sudden implosion of vapor bubbles formed in low pressure regions as they move into high pressure zones in the pump housing. Knowledge of this phenomenon is very important for proper pump design and operation. Some pump designers have defined the critical cavitation coefficient as the point where the operational head drops below the pump performance head characteristic by 3 percent. They generally believe that cavitation could not occur without affecting the operating performance and the onset of cavitation corresponds with the drop of total head. In addition, sustained operation of the pump would lead to cavitation erosion. However, it is possible that cavitation actually commences well the operating performance is affected, and if this is so, then it needs to be considered in effecting better pump design or operating criteria. Good experimental data at the onset of cavitation (both visual and measurable) would be most valuable to improve pump runnability, longevity and performance.

Cdina (2003) measured audible sound levels to detect cavitation in centrifugal pumps. He showed that there is a discrete frequency tone at 147 Hz which strongly depends on the cavitation process and its development. This discrete frequency was used to detect both cavitation onset and development. The net positive suction head required was determined by an alarm at that critical frequency, and was used to prevent pump cavitation by initiating either shutdown or flow throttling.

Alfayez *et al.*, (2005) used an Acoustic Emission (AE) technique to detect incipient cavitation and the best efficiency point of a centrifugal pump. The sensors were located at different positions at the suction and discharge sides. They found that AE activity located in the vicinity of impeller or pump casing has the largest magnitude, and the minimum AE rms value was obtained at a specific flow rate corresponding to the best efficiency point. Based on these observations it was concluded that the BEP must occur at minimal flow turbulence in the system, and hence at minimal AE activity. In this investigation the AE signal was plotted together with the performance curves in order to obtain a better understanding of AE results. However, in some cases there are difficulties installing sensors for monitoring the stability, performance, and detection of cavitation in pumps such as submersible pumps. Alfayez *et al.* (2004) also used the acoustic emission technique and identifying the pump best efficiency point. To avoid these problems, Parasuram *et al.* (2006) presented an experimentally demonstrated sensorless approach for detection of varying levels of cavitation in centrifugal pumps when an induction pump motor is used. This method does not require knowledge of motor or pump model or any detailed design parameters. They used a 2.2 kW induction motor and obtained line voltages and phase currents to detect and record the intensity and level of cavitation.

Corresponding Author: S.N. Kazi, Department of Mechanical Engineering, Faculty of Engineering, University of Malaya, 50603 Kuala Lumpur, Malaysia.

E-mail: salimnewaz@um.edu.my, salimnewaz@yahoo.com

Tel: (603) 7967 4582, Fax: (603) 7967 5317

El-Kadi (2001) studied cavitation in a centrifugal pump handling hot water (from 28 °C to 58 °C) with the suction side made from transparent Perspex. However, they did not correlate the estimated NPSH at the corresponding onset of cavitation, to a drop of 3% total discharge head.

Park *et al.*, (2009) presented a numerical prediction of tip vortex cavitation behavior and noise considering bubble nuclei size and distribution, using a numerical Eulerian–Lagrangian approach. They studied the relationships of cavitation inception, pressure-sound level, and cavitation nuclei size, at several cavitation numbers. They found that at the onset of cavitation, smaller nuclei are more sensitive to the change of cavitation number and cavitation noise, and the smallest nuclei have the most influence on overall tip vortex cavitation noise.

Donald Sloteman (2007) studied cavitation in a high energy centrifugal pump using noise measurements and visualization techniques in order to detect and assess damage potential. Noise-level waveform data from six different sensors positioned very near to each other were examined and flow visualization was facilitated through a transparent window. He found that changes in cavitation level could be measured at many locations in the pump and piping. Finally he concluded that after-market detection tools could be useful for optimizing pump design and in pump manufacturing.

Al-Arabi and Selim *et al.*, (2007) presented a theoretical model for the prediction of the incipient of cavitation in centrifugal pumps. The model includes the physical fluid parameters and the real working phenomena at the off-design condition. The parameters considered in the model were, flow rate ratio, pump rotational speed, water temperature, thermodynamic properties of water, nuclei and gas content, relative velocity and incidence angle. The model showed that the thermodynamic effects were more complex than other parameters. The model has been tested against extensive published experimental results for centrifugal pumps over a wide operating condition. The comparison of the predicted net positive suction head at inception with the published data showed a good agreement.

Zin (2007) and Zin *et al.*, (2006) carried out an experimental study analyzing vibration signals, sound pressure levels, discharge pressure, and flow rates, for feasibility of cavitation detection. They specified three key operating points for a centrifugal pump (Best Efficiency Point BEP, and 90% and 80% of the BEP). They observed that the high frequencies of random vibration in the fast Fourier transform (FFT) spectrum were vital in cavitation diagnosis, and cavitation was found to have easily excited natural frequencies of the pump components.

Experimental:

A schematic diagram of the experimental flow loop is presented in Figure 1. The flow loop is comprised of an electrically-driven, variable-speed pump, piping, an electromagnetic flow meter, valves, and instrumentations. The specifications of the test rig components are presented in Table 1.

- 1- Pump motor
- 2-Pump.
- 3-Delivery valve
- 4-By-pass line
- 5-Electromagnetic flow meter
- 6- Orifice
- 7- Main tank.
- 8-Electric heater
- 9- Main suction valve.
- 10- Control suction valve.
- 11- Speed inverter
- 12 – Suction pressure gauge
- 13 – Delivery pressure gauge
- 14- U-manometer tube

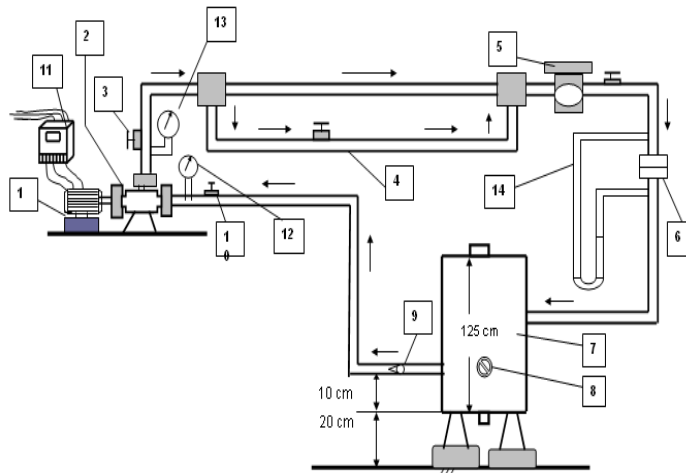


Fig. 1: Cavitation Test Circuit.

Table 1: Specification of test rig components.

Centrifugal pump	Type	Electric motor power	specific speed	Impeller	
	INTERSIGMA (NVA) series, 50 NVA-175-6	5.5 kW	1.87	Type	Closed type
				Inlet diameter	54 mm
				Outlet diameter	175 mm
				Blades shape	Back curved blades
				No. of blades	6
				Blade inlet angle	21.5°
				Blade outlet angle	28°
				Inlet blade height	10.5 mm
Outlet blade height	5 mm				
Main Tank	Volume	Height	Diameter	Wall thickness	
	0.34 m	120mm	600 mm	10 mm	
Speed inverter	Type	Ratio of rotation			
	(Hitachi L100)	(0 – 7) times of pump rotational speed			
Electric heater		Type		Power	No. of heaters
		Glass wool insulated Nicrome		2 kW	3
Suction and delivery diameters		50.8 mm			
Suction and delivery pipes material		Carbon steel			

The transparent perspex pump inlet section is connected to a 43 cm length of 50.8 mm inside-diameter Perspex pipe to enable the swirling waves in the suction side to be observed. The impeller front shroud was manufactured from transparent perspex to permit visual observation of cavitation inception. The outer surface of original impeller was removed gently in order to replace it by a perspex cover. Volumetric flow rate was measured with an electromagnetic flow meter, and which was calibrated using an installed orifice plate with a mercury manometer. A special cooling coil was used to maintain constant temperature. Stroboscopic light focused on the perspex pump enabled visual observation of the inception, development, and breakdown of cavitation. The investigation was performed by a high technique photographic process with a 12-bit CCD-camera and a digital video camera operated in frame integrated mode with a frame-grabber device and both of stroboscopic light source and laser-Light-Sheet-Technique were used for illumination of the object. A Sony digital still camera (Model DSC-S70) was also used for high-definition photography. The photography was made in the stroboscopic light which caused yellow colored appearance of the photographs.

Test Conditions:

The experimental test conditions are presented in Table 2. The suction static lift of 0.67 m was kept constant, and checked repeatedly during the tests. The experiments were carried out at constant room temperature and atmospheric pressure.

Table 2: Experimental test conditions.

Parameter	Unit	Range
Flow rate (Q)	Liter/sec	0.3 – 1.1
Rotational speed (N)	RPM	1500 - 3000
Temperature (T)	°C	20 - 90

RESULTS AND DISCUSSION

Visual Incipient of Cavitation and Net Positive Suction Head:

The onset of cavitation is the first appearance of a limited cavitation zone at the leading edge of the pump impeller blade. Stroboscopic light augments visual discernment so that an estimation of the corresponding net positive suction head ($NPSH_{vis}$) could be made. A relationship between estimated $NPSH_{vis}$ and the NPSH corresponding to 3% drop in head provides pump designers with more accurate criteria of the onset of cavitation for better design practice. An extensive series of experiments were carried out at various operating conditions to obtain these data.

Relation Between Visual NPSH and NPSH Corresponding to 3% Drop in Head:

Cavitation develops with attenuation of performance and the onset of cavitation appears as a sudden drop in total discharge head. Severe cavitation is likely to occur if the head drops by 3%, but the reliance on this concept would cause errors in the prediction of efficiency and performance at the design stage. Therefore, data on the variation of visual observation and corresponding net positive suction head NPSH against for a 3% drop in head at various operating conditions are needed to develop possible relationships between them.

Table 3 shows the reality of cavitation at 3% head drop at a flow ratio $Q/Q_{opt} = 0.4$, various water temperatures and different rotational speeds. Data indicate that the onset of cavitation commences long before the 3% drop in head, and developed cavitation is observed at 3% drop with severe erosion. The length of the

effect of cavitation on the blade varied from 25% to 70% by visual observation at 3% drop in head. Photographs of the effects of cavitation at 3% drop in head are presented in Figure 2.

Table 3: Reality of cavitation according to observation.

Parameters	T [°C]	N (rpm)	Q/Q _{opt}	NPSH _{vis} (m)	NPSH _{3%} (m)	Percentage of cavity length to blade length
P _{suc.} = 0.80 bar, P _{del.} = 2.5 bar H = 33.4 m	20	2800	0.40	8.45	3.12	25 %
P _{suc.} = 0.60 bar, P _{del.} = 3.2 bar H = 38.32 m	20	3000	0.40	8.88	3.85	40 %
P _{suc.} = 0.7 bar, P _{del.} = 2.5 bar H = 32 m	40	2800	0.40	8.44	4.32	50 %
P _{suc.} = 0.52 bar, P _{del.} = 3 bar H = 36 m	40	3000	0.40	9.22	5.5	70 %
P _{suc.} = 0.40 bar, P _{del.} = 3.1 bar H = 35.6 m	70	3000	0.40	6.42	4.9	> 75 %



Fig. 2: Developed cavitation corresponding to 3% drop in head (T = 40°C, Q/Q_{opt} = 0.4, N = 2800 rpm).

The graph of NPSH_i against NPSH_{3%} is shown in Figure 3 (independent of flow rate ratio and rotational speed, but dependent on the water temperature). Good relationships were obtained for all the data.

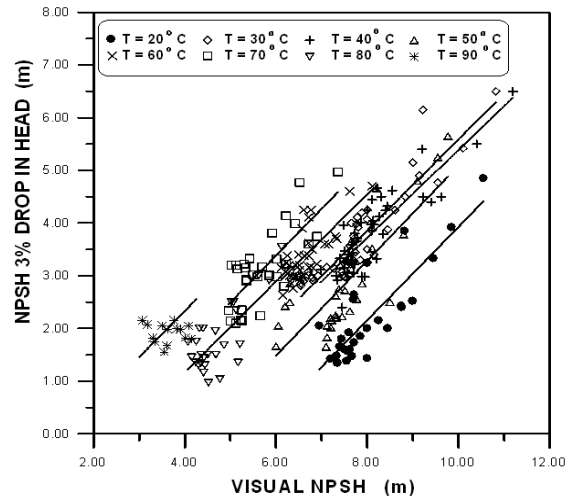


Fig. 3: NPSH_{3%} drop in head versus NPSH_{vis}

The correlation coefficient is best for the affect of temperature, but the others relationships are acceptable for results of this nature. This would seem to be a useful tool for predicting incipient of cavitation in a pump from performance tests, which makes ease to collect cavitation information.

Table 4: The correlation coefficients and regression equations for the lines, derived from Figure 3.

Data	Correlation coefficient		Linear Relationship Equation	
Independent of operating conditions	0.58		NPSH _{vis} = 2.28NPSH _{3%} - 0.966	(Equation 1)
Dependent only on water temperature	Minimum	0.62	NPSH _{vis} = 1.125 NPSH _{3%} - 0.0524 T + 6.3575	(Equation 2)
	Maximum	0.87		

The equations for the regression lines were derived from the data presented in Figure 4, and values of the correlation coefficients and the regression equations presented in Table 4 validate good relationships.

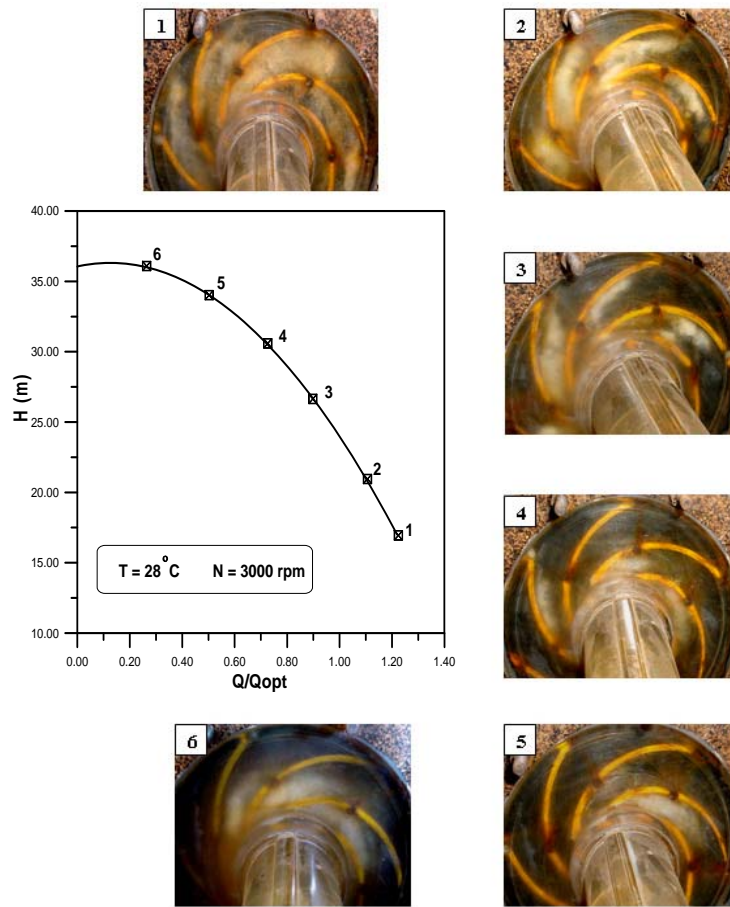


Fig. 4: Visulation of Cavitation at various flow rate ratio at 28 °C and 3000 RPM.

Visual Observation of Cavitation:

Practical difficulties in cavitation testing and obtaining data from the vicinity of a rotating impeller have resulted in limited information, particularly more fundamental insights. Cavitation occurs when vapour bubbles generated in a low pressure zone move into a high press zones and collapse, giving outward pressure pulses and severe noise (vapour bubble implosion). A work programme was conducted using an existing pump rig with a transparent perspex casing for observation and photography, assisted by stroboscopic light. Photographs of cavitation action were obtained under a wide range of discharge throttle settings from wide-open up to the re-circulating condition.

Figure 4 shows a series of photographs taken at various flow rates with constant rotational speed of 3000 rpm and water temperature of 28 °C. At point (1), the delivery valve was fully-open and cavitation was rampant. The bubble collapse phenomena and the resultant ‘shock’ noise and vibration occurred on both suction and pressure sides of the impeller blades, and eventually covered the impeller completely. A reduction in flow rate, point (2), produced a large milky array of bubbles which moved on the surface of the blades, and then travelled with vortex towards the middle of the channel until it reached a point adjacent to the opposite blade. The liquid adjacent to the large-volume zone was observed to contain a multitude of small, travelling transient cavities. With further reduction of flow rate, point (3), the cavitation bubbles decreased in volume with decreasing the flow rate.

The observed cavitation had a milky appearance and the length over which it operated fluctuated. Further reduction in flow rate (point 4) produced cavitation with a fixed sheet attached to the surface of the suction side of the impeller blade. At point 4, the state of alternative cavitation was observed at 70% load. The photograph (point 4) shows there are two cells of fully-developed cavitation on the pressure side within the impeller and they are separated by channel without cavitation. With this observation, it can be understood that an impeller instability problem is driven by the increasing cavity length in relation to the incidence and the start of

recirculation flow at the inlet of the impeller. In this type of cavitation two adjacent channels are operating at different points of the impeller characteristic. The cavitating channel operates at a point with a lower flow rate ratio leading to an increase in the local incidence angle, while the non-cavitating channel operates at a higher flow rate ratio leading to a decrease in the local incidence angle. Consequently the lower flow rate ratio means a stronger pressure rise in the channel between blades and the higher flow rate ratio means a weaker pressure rise. The stronger pressure gradient suppresses the development of cavitation further into the channel while the depression of static pressure rise in the next channel allows cavitation to grow in it. This may confirm Hofmann and Friedrichs experimental results which indicated the occurrence of a periodic cavitation state called “rotating cavitation” in a wide range of part-load conditions (T. C. Zin, 2007).

On further reduction of the flow rate ratio (point 5 and 6), cavitation appears as a cloud of small bubbles and the cloud grows and extends into the impeller passages. This cloud contains small bubbles having glassy appearance. This glassy appearance is due to the growth of gas bubbles by diffusion within the cores of the free vortex which is established outside the boundary layer and surrounding the blade surface. Vortex flows are characteristically, high velocities near the vortex core with corresponding low pressure.

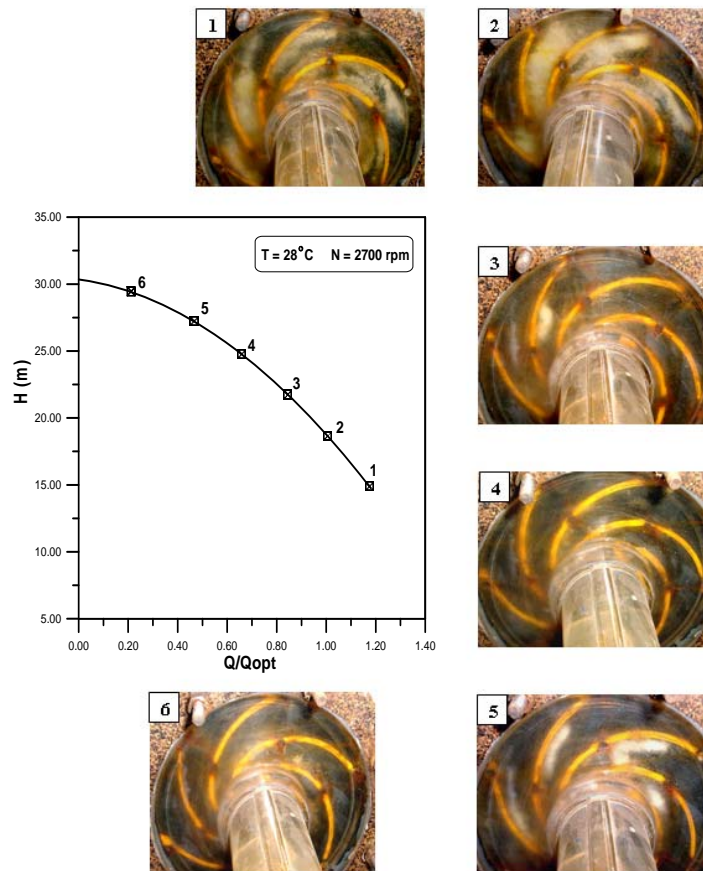


Fig. 5: Visulation of cavitation at various flow rate rations at 28 °C and 2700 RPM.

The photographs in Figure 5 show that the intensity of cavitation increases with increasing rotational speed and is dominated by the re-circulatory flow which increases with increasing rotational speed. With increase of the water temperature to $T = 50^\circ\text{C}$ the colour of the cavities changed gradually and became white with high brightness in colour and the cavities looked like cloud of continuously linked bubbles as shown in Figure 6.

With further increase in the water temperature to $T = 80^\circ\text{C}$ the colour of the cavities had become in-between white and the glassy colour as shown in Figure 7. Also at $T = 80^\circ\text{C}$ the bubbles became elongated in shape and discontinuous clouds were observed as shown in positions 2 and 3 in Figure 7. The photographs show that the cavitation had covered most of the impeller channel at $T = 80^\circ\text{C}$ and $N = 3000\text{ rpm}$ respectively.

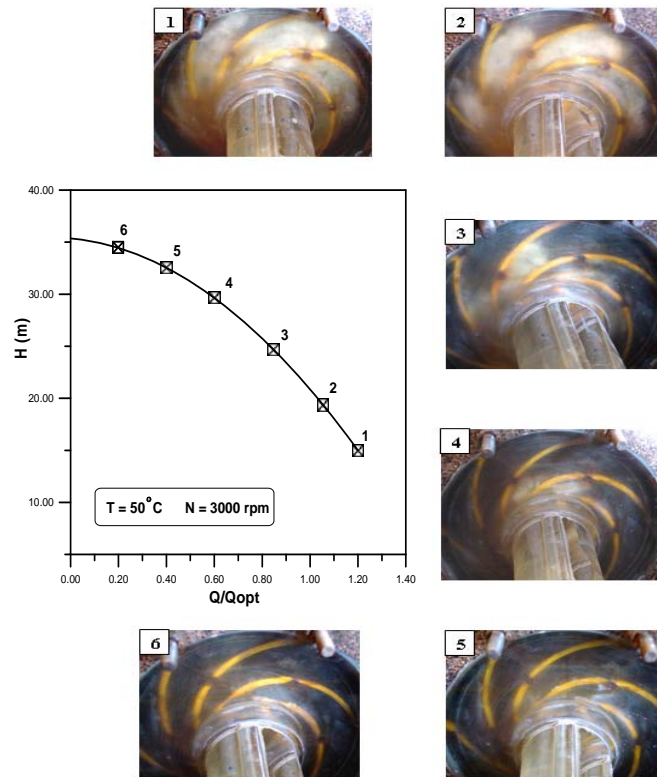


Fig. 6: Visulation of cavitation at various flow rate ratios at 50 °C and 3000 RPM.

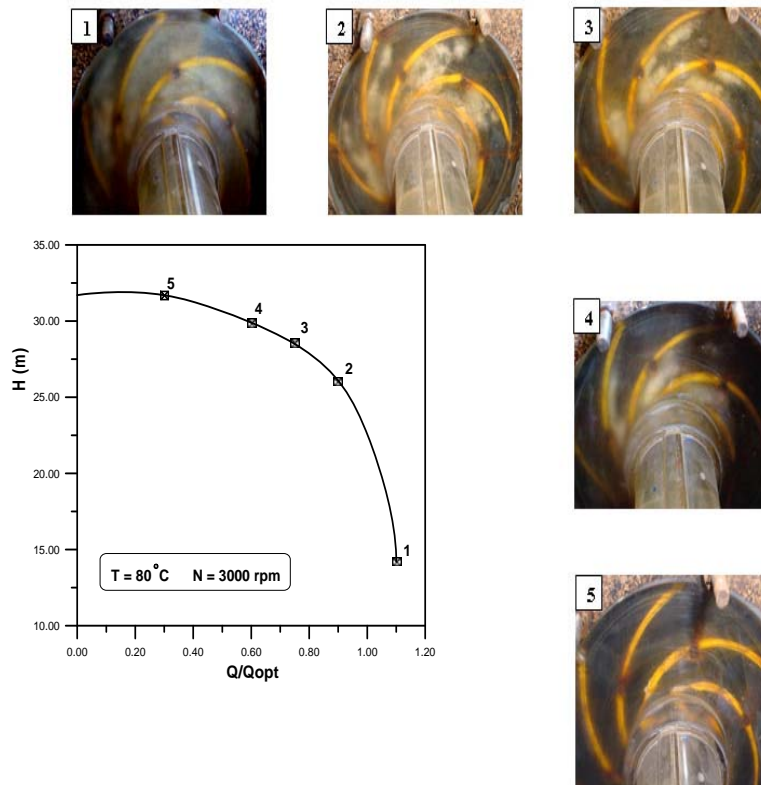


Fig. 7: Visulation of cavitation at various flow rate ratios at 80 °C and 3000 RPM.

Conclusions:

- (i). Visual observation of the cavitation phenomena indicated that cavitation develops at the state where the pump head drops by 3 percent, but the onset of cavitation appears long before the pump performance is affected. At 3% drop of total head severe cavitation is highly likely and design on the basis of that could cause an erroneous prediction estimate of pump performance.
- (ii). Net positive suction head corresponding to the visual onset visual of cavitation ($NPSH_{vis}$) is well correlated with the net positive suction head corresponding to 3% drop in head ($NPSH_{3\%}$) and the fluid temperature. An equation is presented that could predict the actual condition of the incipient of cavitation for a centrifugal pump in performance test stage.
- (iii). Visual observation and photographs of the state of cavitation at various flow rate ratios, temperatures, and rotational speeds showed at high flow rate ratios a porous cavity forms, and at lower flow rate ratios, a gaseous cavity develops. The colour of the cavities changed with change of water temperature. At the brink of circulation flow an alternative cavitation commenced at lower flow rate ratios ($Q/Q_{opt} < 0.5$).

REFERENCES

- Al-Arabi, A.B. and S.M.A. Selim, 2007. A Theoretical Model to Predict Cavitation Inception in Centrifugal Pumps, Proceedings of 5th International Conference on Heat Transfer, Fluid Mechanics and Thermodynamics, Sun City, South Africa.
- Alfayez, L., D. Mba and G. Dyson, 2005. The application of Acoustic Emission for detecting incipient cavitation and the best efficiency point of a 60kW centrifugal pump; case study, NDT & E International, 38: 354-358.
- Alfayez, L., D. Saudi, G. Dyson, D. Browne, 2004. Detection of incipient cavitation and the best efficiency point of a 2.2MW centrifugal pump using Acoustic Emission, Proceedings of 26th European Conference on Acoustic Emission Testing, Berlin.
- Cdina, M., 2003. Detection of cavitation phenomenon in a centrifugal pump using audible sound, Elsevier Science Ltd, 17(6): 1335-1347.
- Donald, P.S., 2007. Cavitation in High Energy Pumps - Detection and Assessment of Damage Potential, Proceedings of the Twenty-Third International Pump Users Symposium, pp: 29-38.
- El-kadi, M.A., 2001. Cavitation in centrifugal pumps handling hot water” Eng. Res. Journal, Helwan University, 77: 200-216.
- Parasuram, P.H. and G.P. Alexander, 2006. Sensorless detection of cavitation in centrifugal pumps, ASME International Mechanical Engineering Congress and Exposition, USA.
- Park, K., H. Seol, W. Choi and S. Lee, 2009. Numerical prediction of tip vortex cavitation behavior and noise considering nuclei size and distribution”. Elsevier Ltd, Applied Acoustics, 70: 674-680.
- Zin, T.C., 2007. An experimental and field study of cavitation detection in pump, Masters thesis, Universiti Teknologi Malaysia.
- Zin, T.C., M.S. Leong and C. Lee, 2006. Field investigation of cavitation and flow induced vibrations in submerged vertical pumps in a power plant, Engineering Asset Management, pp: 1177-1186.